Investigation of the Influence of Array Arrangement and Spacing on Tidal Energy Converter (TEC) Performance using a 3-Dimensional CFD Model

Luolin Bai[1], Roy R G Spence[2] and Grégory Dudziak[2]

[1] Feng Neng Sgurr (Beijing), Wind Analysis Team,
No. 5 Dongzhimen S Ave, Dongcheng, 100007, Beijing, China
E-mail: luolin.bai@sgurrenergy.com

[2] SgurrEnergy, Marine Team, 225 Bath Street, G2 4GZ, Glasgow, UK
E-mail: roy.spence@sgurrenergy.com
E-mail: gregory.dudziak@sgurrenergy.com

Abstract

This paper details work conducted using the commercial CFD software package Fluent to investigate the influence of different TEC array arrangements. This work investigates the performance variation across a TEC located centrally in an array (measured as a pressure differential). Two scenarios were considered. Firstly, we examined the influence on a central TEC of other TECs in a fixed spacing array and for different configurations (single row array, two-row array with turbines upstream of the central TEC, three-row array with turbine rows both upstream and downstream of the central TEC). Secondly, we examined the influence on a central TEC of other TECs for a given three-row array configuration but considering different latitudinal and longitudinal spacings.

This approach to TEC array modelling does not attempt to conduct detailed modelling of the TEC, but instead examines the variation in the performance of a central TEC as the array is increased row by row. Additional modelling work detailing simulations conducted to investigate the influence of chosen model parameters and assumptions are also summarised along with a discussion of related uncertainties.

Results of analyses examining the influence of the lateral and longitudinal MCT spacing are presented for a tidal farm array comprising three rows. This work examines the relative effect of increasing the inter row spacing between TEC turbines from 3 TEC rotor diameters to 5 and the row spacing from 10 TEC rotor diameters to 15.

Keywords: Array, CFD, Spacing, Tidal Energy Converter (TEC).

© Proceedings of the 8th European Wave and Tidal Energy Conference, Uppsala, Sweden, 2009

Nomenclature

C	=	pressure jump coefficient
h	=	sea depth
K	=	turbulence kinetic energy
V	=	velocity
α	=	face permeability
Δm	=	porous media thickness
ε	=	dissipation rate of turbulence kinetic energy
ω	=	specific dissipation rate
d	=	TEC rotor diameter

Subscripts

$mean$	=	mean value
x	=	axial component

1 Introduction

The potential of power generation from marine tidal currents is sizable. High load factors and the spatial and temporal predictability of the tidal resource characteristics make marine currents particularly attractive for power generation opportunities. However, there is still a high level of uncertainty associated with the annual energy production of tidal farms. This is largely caused by the absence of established methodologies and hence software packages to suit these methodologies due to the infancy of the industry and absence of operational tidal arrays. In contrast the more mature wind industry has a number of standard software packages (such as WAsP) and there is a large enough market to support the development of Computational Fluid Dynamics (CFD) based wind only software packages, e.g. Meteodyn, WindSim and Ventos. However, when the current wind related software is found to be inadequate to model specific flow applications [1-2], for example offshore wake modelling in large wind farm arrays [3-5], a number of studies are instigated to enhance understanding and improve modelling techniques [6-7].

While there are similarities between wind and tidal resource modelling applications there are also fundamental differences that prevent a wholesale transfer of methodologies and modelling software. This has resulted in analysts opting to use general CFD flow packages to model the performance of TECs or assess energy extraction potential. These CFD packages can be in-house developments (eg Fluidity) or more commonly commercial codes such as Fluent, CFD and Star-CD. CFD software packages typically require a significantly higher level of user expertise, in depth knowledge of the application, detailed analysis set up, longer solver and post-processing times and increased cost in comparison to wind specific software packages.

It is considered that even with these drawbacks CFD software packages currently offer the best method of modelling the flow features in and around TECs and TEC arrays. The University of Southampton have performed some array related modelling using a 2D boundary layer approach under simulated tidal conditions as well as wake characterisation [8, 9]. This work has involved both experimental and computational work and it is noted that the numerical work has utilised an actuator disk approximation within CFD software, without considering ocean conditions [10]. Strathclyde University have also provided a brief summary of work performed using Fluent where detailed TEC model geometry was analysed [11]. Additionally the University of Napoli have also utilised CFD and the actuator disk approximation to investigate the potential of systems for harvesting tidal current energy [12]. Other modelling work at the University of British Columbia has developed a framework for planning a tidal turbine farm system with vertical axis tidal current turbines [13].

The study presented in this paper aims to demonstrate the current capabilities of 3D CFD software in simulating an MCT array without utilising super-computer processing facilities but achieving the results in a reasonable time frame. This study has been conducted in such a manner to allow two array scenarios to be examined. The first scenario investigates the influence of building up array around a central TEC to observe the influence of the surrounding TECs on the central TEC. The second scenario investigates the influence of the TEC spacing within the array on the overall performance of the array.

This study is restricted to using approximate or indicative values were appropriate. However, to reduce the influence of these approximations all results are presented relative to base case simulations.

2 Description of Model

Constructing a TEC array model is a complex task and in order to achieve this in a reasonable timeframe using publically available data a number of assumptions were made. These assumptions will be highlighted as each element of the model construction is discussed. The model was simulated using the ANSYS: Fluent software package.

Computational Domain

SgurrEnergy has previously conducted investigations into the influence of the seabed bathymetry data on the tidal flow. However, it was decided that in order to simplify the computational model and to remove the bathymetry effect from the different array arrangement simulations, a flat seabed profile would be used.

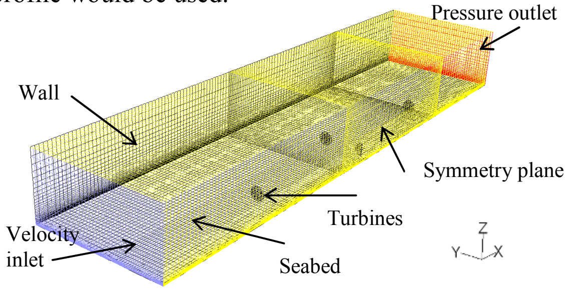

Figure 1: Computational domain

Again from previous experience the basic domain was sized at 650m long (X-axis) by 400m wide (Y-axis) by 100m deep (Z-axis). However the domain dimensions were varied for different array sizes to ensure that there were a minimum of 10 rotor diameters from the inlet to the first row of turbines and a minimum of 10 rotor diameters from the last row of turbines to the domain output for all analyses. The distance between the domain side and the nearest lateral turbine was also a minimum of 10 rotor diameters. The influence of the width of the domain on the TEC output is investigated in Section 4. The computational domain is shown in Figure 1.

Grid

The computational domain was created using a hybrid mesh that consisted of both hexahedrons and tetrahedron prisms. Twelve boundary layers extruded from quadrilateral meshes at the bottom are attached at the seabed with the bottom mesh layer depth being 0.1m with an aspect ratio of 1.1. The total height of boundary layers is about 3.6m and contains a total of 14 layers. The number of elements in width, length and depth is about 80x140x40. The total model mesh size is around 450,000 elements. An indication of the computational mesh is provided in Figure 2.

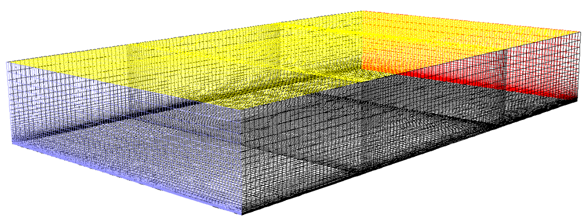

Figure 2: Computational domain surface mesh

Boundary Conditions

The boundary conditions employed for this study are summarised below. The bulk of these are relatively standard for incompressible, viscous fluids.

Inlet: Velocity profile
Outlet: Constant static pressure
Sidewall: Zero stress wall condition
Seabed: No slip wall condition
Water Surface: Symmetry plane

The inlet velocity condition was applied with a User Defined Function (UDF) in FLUENT with an average velocity of $3ms^{-1}$ with a $1/7^{th}$ power law profile.

The 1/7th power law profile used is shown in Figure 3, where V_x is the axial inlet velocity, $V_{mean}=3.0ms^{-1}$, h=100m (sea depth):

$$V_x = V_{mean}\left(\frac{Z}{0.32h}\right)^{1/7} \quad (1)$$

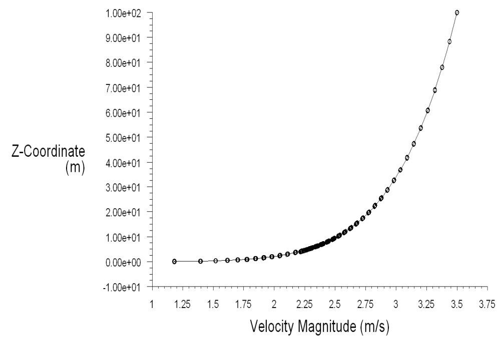

Figure 3: Velocity inlet profile

The zero stress wall conditions are applied to reflect a free stream fluid flow at the sidewall boundaries. The free surface of the fluid is modelled as a symmetry boundary condition. The turbulence intensity at inlet and outlet is set as 5%.

The use of a symmetry plane for the surface of the water is commonly employed where surface effects will not influence the analysis. For this model the distance from the rotor tip to the water surface is 70m and so surface effects are not significant.

Tidal Energy Converter

A decision was taken to base the TEC on a Horizontal Axis Turbine (HAT). Examining publically available data, a rotor diameter of 20m and a hub height of 20m were considered to be reasonably representative of current HAT technologies.

Conducting detailed analyses of a single specific TEC is problematic as this requires detailed turbine design and performance information which is likely to be commercially restricted. An equivalent actuator disk model representing a real turbine in a three dimensional CFD model offers an economically viable analysis tool, in terms of mesh size and solution timescales, for assessing turbine response in a range of conditions and environments [14-15]. Thus the TEC was modelled in the computational domain as an actuator disk. The actuator disk model in FLUENT represents rotor blades with momentum sources allowing a pressure differential to exist across the disk. This reduces the mesh size and generation time to create a domain inclusive of a turbine model. However the actuator disk approximation cannot account for the transfer of rotational momentum. The parameters applied in Fluent for the actuator disk model are summarised below:

Face permeability (α): $1x10^{10}m^2$
Porous media thickness (Δm): 0.5m
Pressure jump coefficient (C): $25m^{-1}$

The permeability of the disk was set to a high value of $10^{10}m^2$ to cancel out viscous effects and account only for the effect of friction. Porous media thickness was set to be 0.5m which was thought to be a good approximate value for the thickness of the TEC's rotor. A value for the pressure jump coefficient of $25m^{-1}$ was set as a constant throughout. The pressure jump coefficient was based on presumption that the porous plate has 20% area open to flow. The derivation of the pressure jump coefficient can be found in FLUENT help documentation [16].

Solver Control and Turbulence model

A first order discretisation scheme was used for the convergence. While sacrificing some accuracy they allow robust and rapid convergence of the iterative solution.

The model utilised the shear-stress transport (SST) $K-\omega$ turbulence model for the simulations. The SST $K-\omega$ model was developed to effectively blend the robust and accurate formulation of the $K-\omega$ model in the near-wall region with the free-stream independence of the $K-\varepsilon$ model in the far field [17]. The SST $K-\omega$ model is more accurate and reliable for a wider class of flows including adverse pressure gradient flows than the standard $K-\omega$ and $K-\varepsilon$ models. Figure 4 shows how turbulence dissipates in the wake region.

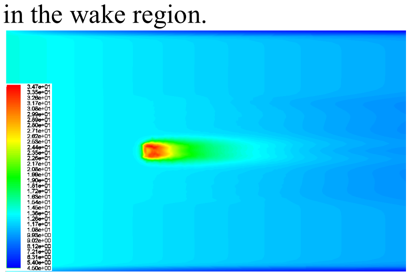

Figure 4: Turbulence intensity distribution in wake region

3 Model Investigations

Symmetrical plane

The model employed for this study utilises a symmetry boundary condition along the central vertical plane. Thus, as illustrated in Figure 5 the analysed model size is half of the simulated case as the simulated case includes the mirrored section due to the symmetry boundary condition.

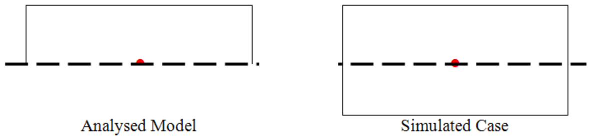

Figure 5: Central symmetry boundary condition along a vertical plane

The use of this symmetry plane produces significant savings in terms of model size and therefore computation time. However as the plane intersects with the position of the central TEC it is important to gauge the influence of this model boundary on the results. Therefore two models were analysed. The first examined the model utilising a symmetry boundary condition and the second a model, twice the size of the first, with no symmetry boundary. Apart from the model size and the use of a symmetry boundary condition all other analysis parameters were kept consistent between the analyses including the actuator disk model of the TEC.

A comparison of the two analyses indicated that there was a small variation whereby the symmetry model under predicted the pressure drop resulting from the actuator disk by 0.54%. This loss of accuracy in the simulation caused by the inclusion of the symmetry boundary condition is considered acceptable.

Domain width

Experience with TEC analyses has indicated that the domain width could influence the computational results. The sidewall boundary conditions, while representing a freestream flow condition could potentially have the effect of constraining slightly more fluid through the device than would occur in a very large or completely free domain. Generally the ratio of the TEC rotor diameter to the domain size is generally considered as a blockage factor. So the smaller the domain size, the larger the blockage factor, which will cause the modelled fluid velocity through the rotor to artificially accelerate resulting in an overestimation of the TEC power.

To examine the influence of the domain size the fluid flow was examined for three domain widths (400m, 800m and 1200m). All three computational models use the central symmetry boundary condition and a three TEC row configuration (See Section 4 for model configurations). An image of the velocity contours in the three domains is shown in Figure 6.

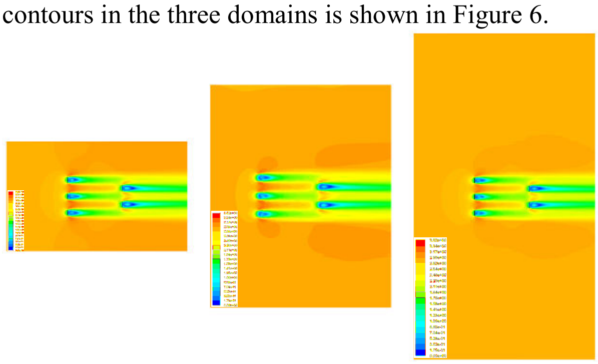

Figure 6: Comparison of velocity contours with different domain width

It is observed that the velocity contours close to the TEC and in the wake region are very consistent. After checking the velocity at the centre of the central turbine, it is found that the difference of velocity is very small; the variation is within 0.5%. Based on this fact, a conclusion can be drawn that a 400m domain width (20 TEC diameters) is appropriate. However there is variation in the wider flow field. Comparing the pressure drop across the central TEC for the three domains indicates that there is less than a 0.5% variation from the smallest domain to the largest. It is noted that the relationship between the domain size and the level of error is non-linear with the double size domain showing a variation of around 0.4% variation in the pressure drop. This, again, is considered an acceptable level of error for the significant improvement in mesh size and solution.

4 Model Configurations

The TEC array computational model was used to examine two scenarios, firstly examining the influence of surrounding TECs in an array on a central TEC and secondly the influence of spacing within the TEC array. It should be noted that the configurations illustrated in this section are presented with the mirrored portion shown (due to the use of a central boundary condition). The various configurations examined within these scenarios are discussed below:

Scenario 1: Surrounding TEC influence

This scenario examined the influence of other TECs in an array on a central TEC. This was achieved by conducting four analyses that build up each part of a seven TECs, three-row array. The four configurations are as follows:

1. A base analysis with the central TEC only
2. A single array row consisting of three TECs
3. A two-row array, with a two-TEC row located downstream of a three-TEC row.
4. A three-row array consisting of a two-TEC row located upstream of the previous two rows.

The four configurations are shown in Figure 7 where TECs are shown as black dots and the central TEC is shown in red. It should be noted that these images are not to scale and are only indicative of the layout configurations.

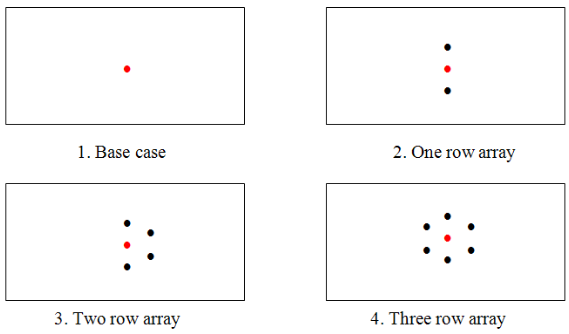

Figure 7: Scenario 1 Configurations

Scenario 2: TEC Array Spacing

The second scenario examined the influence of TEC array row spacing and intra-row spacing on the performance of the TEC array as a whole. Lateral spacing is varied from 3d to 5d and longitudinal spacing from 10d to 15d (where d is rotor diameter). Again the scenario consisted of four configurations that are described below (note configuration numbering is continued from Scenario 1 above):

4. 3d x 10d
5. 3d x 15d
6. 5d x 10d
7. 5d x 15d

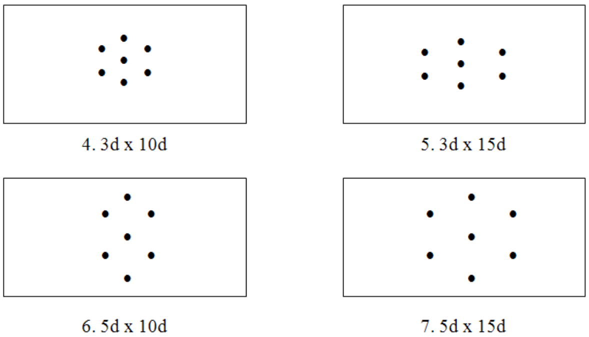

Figure 8: Scenario 2 Configurations

The four configurations are shown in Figure 8 where it should be highlighted that these images are not to scale and are only indicative of the layout configurations. Configuration 4 is common to both scenario 1 and scenario 2.

5 Results

Scenario 1: Surrounding TEC influence

The results for the four configurations related to the build up of a TEC array are shown in Table 1. This table provides the variation in flow rate at the central TEC for each configuration and a comparison of the central TEC power with the base case. It should be noted that a positive flow rate variation corresponds to flow acceleration (and for these configurations increased power extraction). The indicative TEC power is computed from the volume flow rate (in m^3s^{-1}) passing through the actuator disk multiplied by the pressure drop (Pa) across the disk.

Configuration		No. TECs	Variation in Flow (%)	TEC Power (%)
1	Base case	1	Base case simulation	
2	3d	3	2.0%	7.0%
3	3d x10d	5	1.8%	6.4%
4	3d x10d	7	-1.2%	-1.4%

Table 1: Influence of surrounding TECs on central TEC performance

The results indicate that, even when considering the flow rate differences, adding additional TECs in a row (configuration 2) does create a blockage effect that causes a net increase in the output power of the central TEC. For the specific configurations simulated there is a 7.0% increases in power for configuration 2 compared to configuration 1. The addition of a second row downstream (configuration 3) reduces this value slightly indicating that a second (lesser) downstream blockage has little upstream effect. In contrast an upstream row in the array (configuration 4), when flow rate modifications are included, removes any benefit from the blockage effect and provides a result that is quite similar to the base case power output value. This is obvious caused by the interaction of the central TEC with the wakes of the upstream TECs causing a lower velocity at the central TEC.

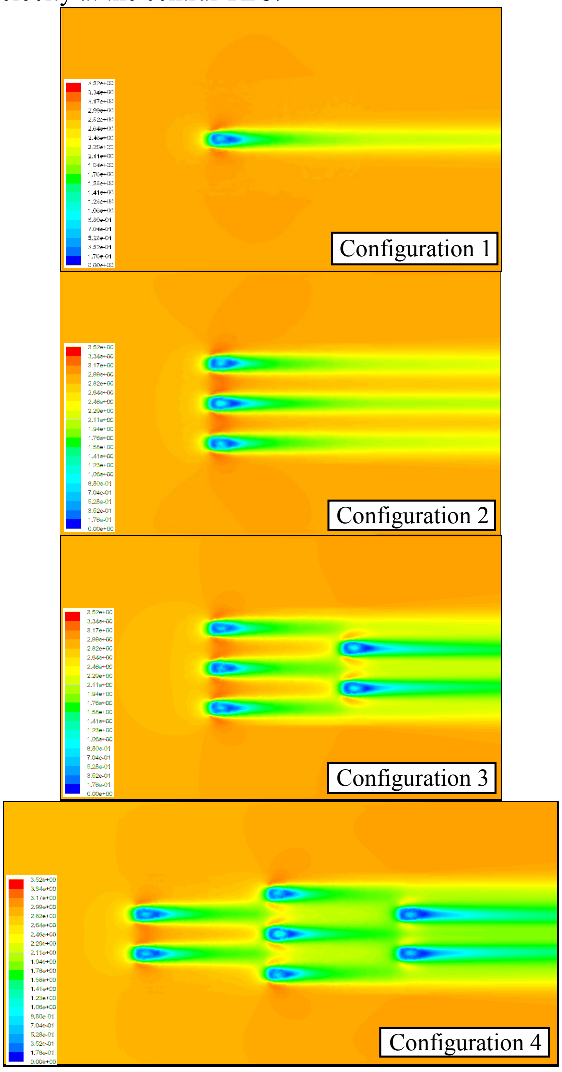

Figure 9: Velocity contours at hub height for three configurations

Figure 9 shows the variation of velocities in the model for three different array configurations. The images have been sized to provide a consistent scale across all configuration outputs. It is noted that configuration 4 uses a longer domain that the previous configurations.

This figure shows the significant wake modelled and that the wake appears to extend well beyond the outlet boundary. The multi-row array simulations show the upstream wakes being truncated by the downstream row. The contours also identify that the TECs in the last row of an array exhibit physically larger wake sizes with the flow within the wakes being slower (darker blue region). This pattern is shown for both two and three-row array configurations. It is also observed for configuration 4 that the wake of the central TEC is physically larger than either of the other two in the central row.

Scenario 2: TEC Array Spacing

In a similar manner to the results presented above, the output from simulations examining the influence of latitudinal and longitudinal spacing is shown relative to the performance of the central TEC. A summary of the output for different TEC spacing within a seven TECs, three rows array is shown in Table 2

Configuration		No. TECs	Variation in Flow (%)	TEC Power (%)
4	3d x10d	7	Base case simulation	
5	3d x15d	7	-0.8%	-8.0%
6	5d x10d	7	1.6%	1.3%
7	5d x15d	7	4.1%	-7.4%

Table 2: Influence of spacing on central TEC performance

The results appear to be counter intuitive, as one may have expected that the larger the spacing the better the TEC performance. However it is important to note that these results are only for the central TEC only and are not indicative of the general array performance.

It is known from the Configurations 1-4 study that the addition of the downstream TEC row decreases the flow through the central TEC. Therefore it seems reasonable that configuration 5 shows a reduction in flow at this TEC when the longitudinal array spacing is increased. Both of the larger latitudinal spacing analyses show increase in the flow through the central TEC. This is perhaps counter intuitive with the previous results (which indicated a flow increase (configurations 1 and 2) when a single TEC operation was compared to a row of TECs. However as can be seen from Figure 10 the larger width spacing arrays shows the fluid entering the central TEC to be influenced less by the wakes from the upstream TEC row. This variation in performance highlights that there is an opportunity to adjust spacing to optimise array performance.

It is surprising that the two largest longitudinal spacing results (configuration 5 and configuration 7) are significantly lower than the other analyses. The explanation for this is not immediately obvious as standard reasoning would predict improved performance for an array with larger spacing. It may be that there is a trade-off between blockage effect and TEC spacing (i.e. wake recovery) that requires more detailed examination than is possible within the restrictions of this study. Verification of the computational model with experimental data is required to determine if this phenomenon is due to the model approximations or if it is an actual flow feature. However it is considered that as the distance from the last array row to the outlet boundary being consistent in all cases and the domain comparisons earlier show only a minor influence, these model parameters are unlikely to be the source of a model error. It should be noted that the outlet boundary, while being a consistent distance from the last TEC row for all configurations, is too close and does not allow reasonable dissipation of the TEC wakes prior to the boundary.

Velocity contours from all four cases in this second study are shown in Figure 10. These plots are taken as a horizontal slice through the model at hub height. Again the domains have been size to ensure consistency of domain dimensions across all configurations shown in the plot. The figure clearly highlights the different domain dimensions used to maintain consistency in the distance from the TECs on the extremities of the array and the model boundaries.

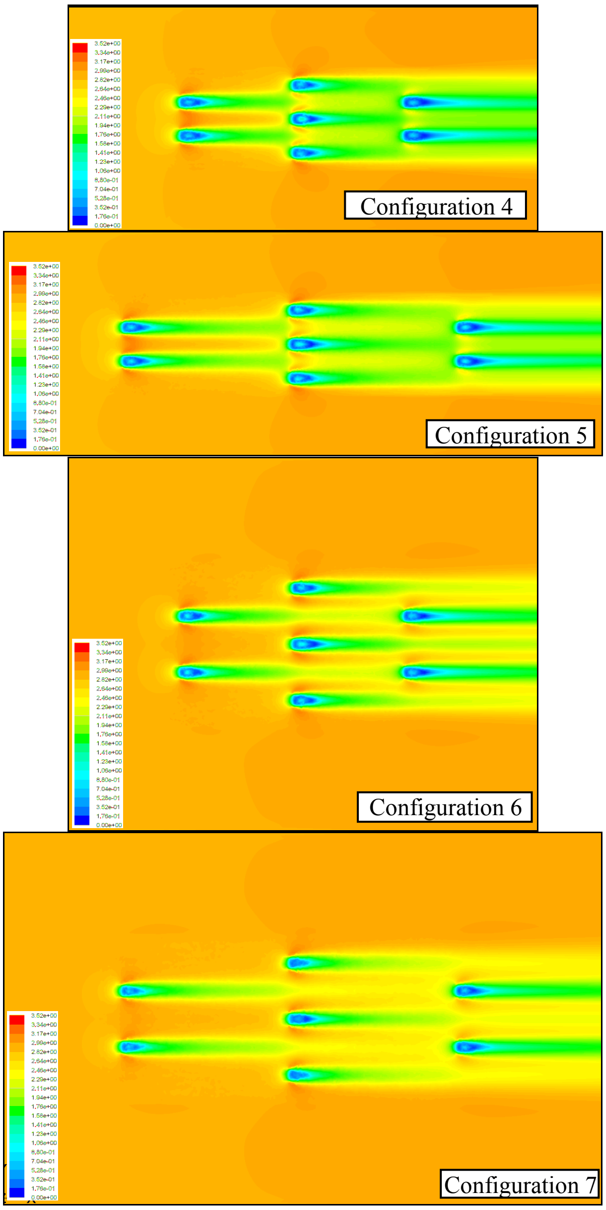

Figure 10: Velocity contours at hub height for four configurations

As observed previously the wakes associated with the last array row are more severe than elsewhere in the array. It is also of interest to note that, for the arrays with the larger latitude spacing, there is less mixing of the TEC wakes. The results for configurations 6 and 7 both show the wake from the leading row passing between the centre row TECs and reaching the final row in the array. The centre row appears to limit the passage of the slowest elements of the wakes downstream.

6 Conclusions

Due to the complexity of the problem and the limited TEC related data available a number of significant approximations and assumptions have had to be made in order to allow the analysis of the influence of individual parameters. This limits the direct usefulness of the data, but comparisons with base case simulations allow the relative influence of TEC array changes to be presented. Thus the study has provided indications on the influence of additional TECs in an array both upstream and downstream. The work has also examined the relative differences in the spacing of the array on a central TEC. The results show that there are significant downstream wake and TEC interactions that are of interest. There are also indications that there are opportunities for optimisation of the array performance through the use of this type of analysis.

The assumptions and approximations made during this study provide immediate avenues for further work. This work will refine both the model and the analysis methodology. However the work shows clearly the capabilities that CFD can provide to the siting of TEC devices and assessing the wake interactions.

References

[1] Gerard Schepers. Flow and wakes in complex terrain and offshore: Model development and verification in UpWind, Energy Research Centre of the Netherlands (ECN), United Kingdom, In *European Wind Energy Conference and Exhibition 2007*

[2] Crespo, A., J. Hernandez, and S. Frandsen. Survey and modelling methods for wind turbine wakes and wind farms. *Wind Energy*, 1999. 2: p. 1-24.

[3] Mechali, M., L. Jensen, R. Barthelmie, et al. Wake effects at Horns Rev and their influence on energy production. In *European Wind Energy Conference and Exhibition*. 2006. Athens, Greece: p. 10.

[4] Barthelmie, R.J., L. Folkerts, K. Rados, et al.. Comparison of wake model simulations with offshore wind turbine wake profiles measured by sodar. *Journal of Atmospheric and Oceanic Technology*, 2006. 23(7): p. 888-901.

[5] W. Schlez, A. Umaña, R. Barthelmie, G. Larsen, K. Rados, B. Lange, G. Schepers and T. Hegberg. ENDOW: Improvement of Wake Models within Offshore Wind Farms. *Wind Engineering* Volume 25, NO. 5, 2001 P P 28 1–287

[6] *UpWind Integrated Project*: Finding design solutions for very large wind turbines. Funded by the EU under Sixth Framework Programme (FP6).

[7] *Carbon Trust Offshore Wind Accelerator Programme*, Key topic Wake Effects.

[8] Blunden L.S. and Bahaj A.S. Effects of tidal energy extraction at Portland Bill, southern UK predicted from a numerical model. *Proceedings Seventh European Wave and Tidal Energy Conference, Porto*, Portugal, 11-14 September 2007.

[9] Bahaj A.S., Myers L.E, Thomson M.D. and Jorge N., Characterising the wake of horizontal axis marine current turbines, *Proceedings Seventh European Wave and Tidal Energy Conference, Porto*, Portugal, 11-14 September 2007.

[10] Batten W.M.J. and Bahaj A.S. CFD simulation of a small farm of horizontal axis marine current turbines. *Proceedings World Renewable Energy Congress (WREC-IX)*, Florence, 19-25 August 2006.

[11] J.A. Clarke, G.Connor, A.D. Grant, C.M. Johnstone, and D. Mackenzie. Development of a Contra-Rotating Tidal Current Turbine and Analysis of Performance. *Proceedings Seventh European Wave and Tidal Energy Conference*, Porto, Portugal, 11-14 September 2007.

[12] D.P. Coiro. Numerical and experimental investigation on novel systems for harvesting tidal current energy. *Ocean Renewable Energy Group Symposium*, Quebec City 21-22 April 2008.

[13] Ye Li, Barbara, J.L., Sander, M.C. Modeling tidal turbine farm with vertical axis tidal current turbines, *Systems, Man and Cybernetics, 2007. ISIC. IEEE International Conference* on Volume, Issue, 7-10 Oct. 2007 Page(s):697 – 702

[14] David Hartwanger, Andrej Horvat. 3D modelling of a wind turbine using CFD. *NAFEMS Conference 2008*, United Kingdom

[15] Mikkelsen, R. *Actuator Disk Methods Applied to Wind Turbines*. Dissertation, Technical Uni. of Denmark, Fluid Mechanics, Dept. of Mech. Eng.

[16] ANSYS: *FLUENT User Guide documentation*: Chapter’s 7.19 Porous Media Conditions and 7.22 Porous Jump Boundary Conditions.

[17] Menter, F.. Innovative Turbulence Modeling: SST Model in ANSYS CFX. *Online document http://www.ansys.com/assets/tech-briefs/cfx-sst.pdf last accessed 9/4/2009.*